Supporting Information

Electrocatalytic Activity of PtAuPd/C Nano Multi-Principal Element Alloy Catalyst towards Oxygen Reduction Reaction

Hui Li [a], Zhiwei Zhang [a], Lianke Zhang [a], Hualiang Ni [a], Haiying Qin [a, *], Jing Zhang [b, *], Hongzhong Chi [a], Junjing He [a]

[a] New Energy Materials Research Center, College of Materials and Environmental Engineering, Hangzhou Dianzi University, Hangzhou 310018, PR China

[b] School of Materials Science and Physics, China University of Mining and Technology, Xuzhou, 221008, China

1. Experimental

1.1 Synthesis of Catalysts

To prepare PtAuPd/C, a mixture solution was prepared by dissolving 0.01 mmol each of $HAuCl_4 \cdot 4H_2O$, $H_2PtCl_6 \cdot 6H_2O$, and $PdCl_2$, in 25 mL of ethanol, and then 80 mg of BP2000 carbon powder was added into the solution. For the preparation of PtAu/C and PtPd/C, solutions containing the corresponding metal salts in the same molar concentration and volume were used, maintaining the same carbon-to-solution ratio. Each mixture was subjected to ultrasonication for 30 mins to ensure uniform dispersion of the metal precursors and the carbon support. Subsequently, the mixture was magnetically stirred at room temperature for 2 hours. Following this, 30 μL of a 5 wt.% Nafion solution was added to each mixture and stirring was continued to produce a homogeneous ink. The resulting ink was uniformly coated onto a 4 cm × 5 cm carbon cloth substrate. After drying, the coated carbon cloth was cut into several 1 cm × 1.5 cm rectangular pieces and fastened onto the carbothermal shock device designed and constructed by our research team. A detailed schematic of the carbon thermal system equipment was previously reported in our work[1]. The carbon thermal shock sintering was conducted at 760 ℃ in an air atmosphere. The catalysts obtained through this pyrolysis process were denoted as PtAu/C, PtPd/C, and PtAuPd/C, respectively.

1.2 Characterization

Infrared thermometry (Optris, CT3MH3 CF) was employed to monitor temperature fluctuations during the carbothermal shock process. Powder X-ray diffraction (XRD) patterns were collected using a MinFlex 600 diffractometer with Cu

Kα radiation (λ = 1.54 Å). The structural and morphological properties of the samples were characterized by transmission electron microscopy (TEM, Talos F200S). Energy-dispersive X-ray spectroscopy (EDS) was utilized to analyze the elemental distribution of the catalysts within dark-field TEM image. The surface chemistry of the catalysts was investigated using X-ray photoelectron spectroscopy (XPS) with an ESCALAB 250Xi XPS analyzer manufactured by Thermo Fisher Scientific (USA). X-ray absorption fine structure (XAFS) spectra at the Pt/Au L-edge were recorded at the beamlines BL11B and BL15U of the Shanghai Synchrotron Radiation Facility (SSRF). The incident photons were monochromatized using a Si (111) double-crystal monochromator. The energy calibration was performed using an individual reference foil. The reference spectra were measured in the fluorescence mode.

1.3 Electrochemical Measurement

The oxygen reduction reaction (ORR)electrocatalytic performance were evaluated on a CHI730e electrochemical workstation at room temperature using a standard three-electrode system. The catalyst ink was prepared by dispersing 8 mg of catalyst powder in a mixture of 1.55 mL of ethanol and 50 μL of Nafion solution (5 wt%). The resulting ink was sonicated for over 30 mins. A specific amount of the catalyst ink was then drop-cast onto a polished glassy carbon disk electrode (RDE, 0.196 cm^2) or a platinum ring-glassy carbon disk electrode (0.247 cm^2), followed by drying at room temperature. The catalyst loading was maintained at 200 μg cm^{-2}. A platinum wire was served as the counter electrode, and a saturated calomel electrode (SCE) was used as the reference electrode. The electrolyte was 0.1 M KOH solution. Unless otherwise noted, reference potentials were given relative to the reversible hydrogen electrode (RHE). The conversion of SCE potential to RHE potential was carried out by equation (1) [2].

$$\mathrm{E}(\mathit{vs.}\ \mathrm{RHE})=\mathrm{E}(\mathit{vs.}\ \mathrm{SCE})+0.0591\times\mathrm{pH}+0.244 \tag{1}$$

Cyclic Voltammetry (CV) measurements were conducted at a scan rate of 10 mV s^{-1} within the potential range of 0.2 to 1.2 V (*vs.* RHE), under O_2 or Ar saturation electrolyte. A 95% IR auto-compensation was applied prior to the testing process. The electrochemical active surface area (ECSA) of the catalysts was determined through the CV measurements, where CV curves were recorded in the non-Faradaic potential region of 1.1-1.3 V *vs.* RHE at various scan rates (10, 20, 40, 60, and 80 mV s^{-1}). The double-layer capacitance (C_{dl}) was calculated from the slope of the linear plot of the current density at 1.2 V *vs.* RHE against the scan rate. The active area was subsequently calculated using Equation (2) [3].

$$\mathrm{ECSA}=\frac{C_{dl}}{C_s} \tag{2}$$

where C_s was the capacitance constant value of a standard flat plate of 1 cm^2, which was taken as 40 μF cm^{-2} in this paper.

Linear sweep voltammetry (LSV) curves were recorded at a scan rate of 10 mV s^{-1} in the potential range of 0.2-1.2 V *vs.* RHE at different rotation speeds (400, 625, 900, 1225, 1600, 2025, and 2500 rpm). The number of electrons transferred (n) during the ORR process was determined from the Koutecky-Levich (K-L) equation (3) [4].

$$\frac{1}{i}=\frac{1}{i_k}+\frac{1}{i_d}=\frac{1}{i_k}+\frac{1}{0.2nFC_0D_0^{2/3}v^{-1/6}\omega^{1/2}} \tag{3}$$

Specific activity（SA, mA cm^{-2}）was the kinetic current normalized to the active surface area, obtained by dividing i_k by the ECSA, using Equation (4) [5].

$$\mathrm{SA}=\frac{i_k}{\mathrm{ECSA}} \tag{4}$$

The rotating ring-disc electrode (RRDE) test was performed at a rotational speed of 1600 rpm. The electron transfer number (*n*) and the hydrogen peroxide (H_2O_2) yield could be determined from Equations (5 and 6) [6].

$$\mathrm{n}=4\times\frac{I_d}{I_r/N+I_d} \tag{5}$$

$$\mathrm{H_2O_2}(\%)=200\times\frac{I_r/N}{I_r/N+I_d} \tag{6}$$

The ORR stability of the electrocatalysts was examined in accelerated durability tests (ADT) between 0.7 and 0.8 V (*vs.* RHE) for different cycles at a scan rate of 50 mV s^{-1} for 10,000 or 40,000 cycles, in O_2-saturated 0.1 M KOH solution without replenishment strategy.

1.4 Fuel cell performance test

A PFX-2011 cell tester (Kikusui Electronics Corp) was employed to investigate the cell performance, tested at 30 and 60 °C. The catalyst loading was 5 mg cm^{-2}. The cathode catalyst was prepared by mixing the synthesized catalyst with a Nafion solution (5 wt.%) at a 1:7 mass ratio. The anode catalyst was prepared by combining $Co(OH)_2$-PPy-BP catalyst, Nafion solution (5 wt.%), and ethanol in a 1:7:3 mass ratio. The electrolyte membranes were Nafion 117 and Nafion 212. The membranes were pretreated by boiling in a 3 wt.% H_2O_2 solution followed by boiling in deionized water, each for 1 hour. A 5 wt.% $NaBH_4$ solution containing 10 wt.% NaOH was used as the fuel with a flow rate of 30 mL min^{-1}. Humidified high-purity oxygen was supplied as the oxidant at a flow rate of 100 mL min^{-1} and a pressure of 0.25 MPa.

2. Supplementary Figures and Tables

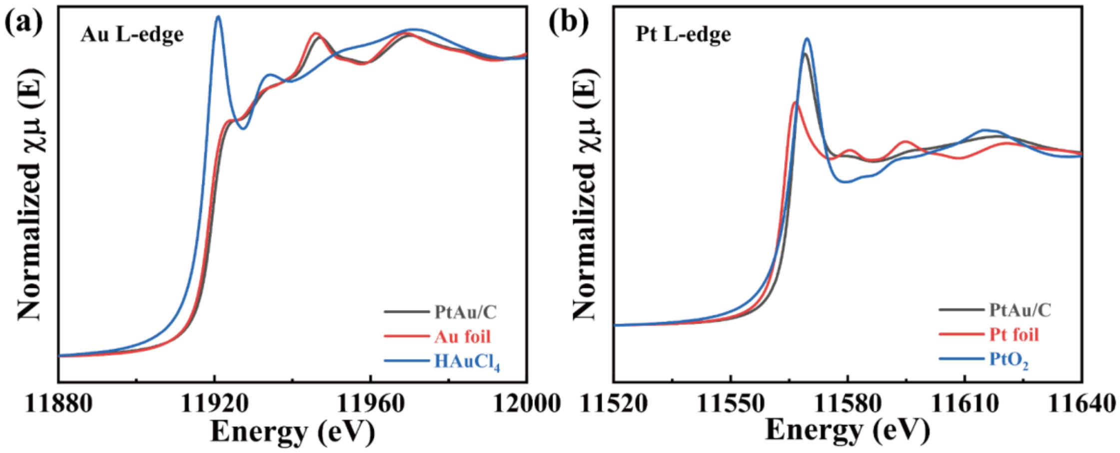

Fig. S1. XANES spectra of PtAu/C catalyst: (a) Au L-edge and (b) Pt L-edge.

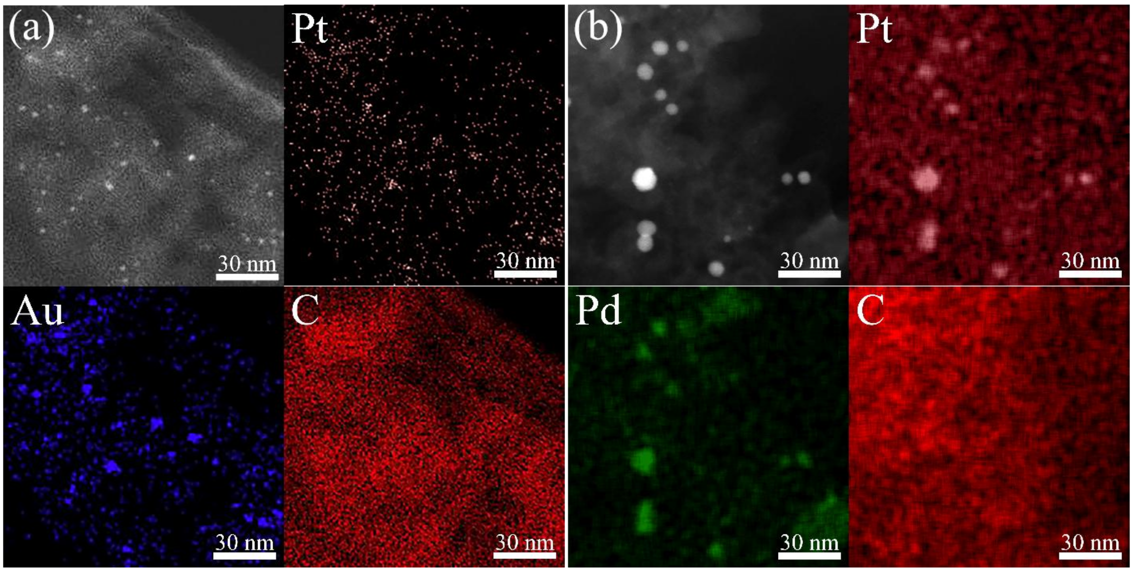

Fig. S2. Mapping element distribution diagrams: (a) PtAu/C and (b) PtPd/C after electrified sintering.

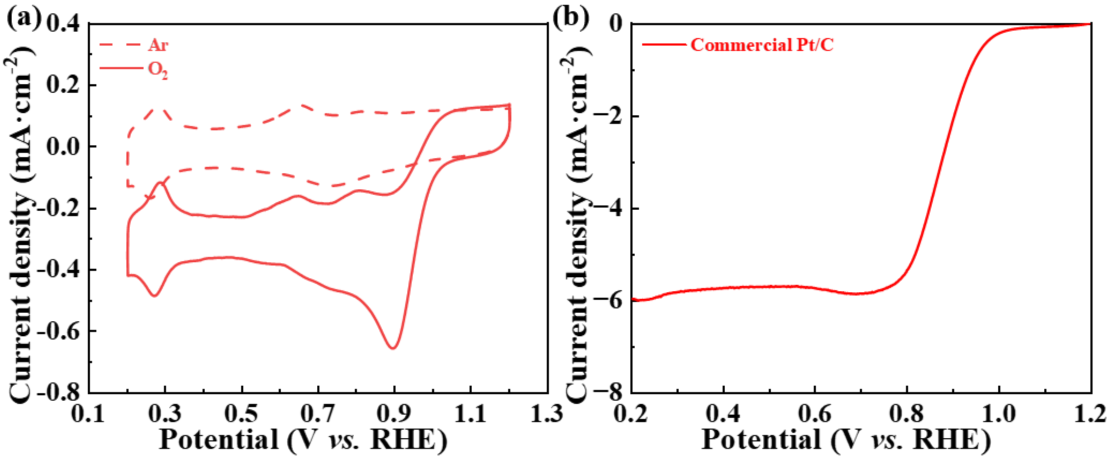

Fig. S3. (a) CV curves under saturated oxygen and saturated argon, and (b) LSV curves at 1600 rpm of commercial Pt/C.

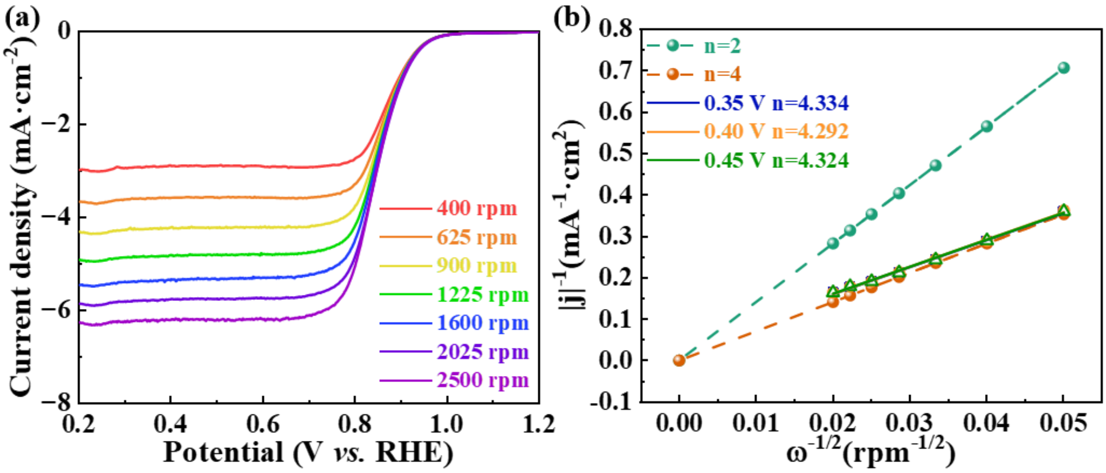

Fig. S4. (a) LSV curves at 400-2500 rpm and (b) transfer electron numbers at 0.35, 0.40 and 0.45 V calculated by the Levich equation of commercial Pt/C catalyst.

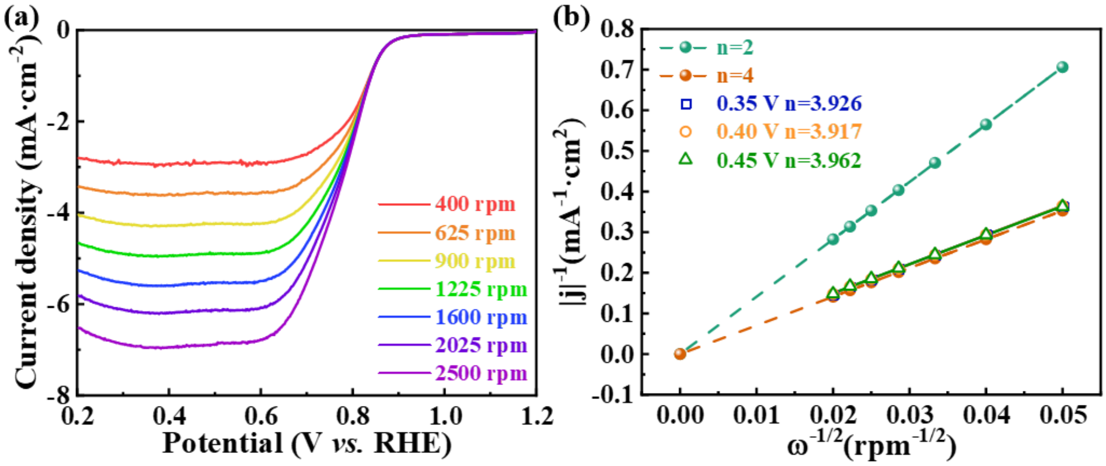

Fig. S5. (a) LSV curves at 400-2500 rpm and (b) transfer electron numbers at 0.35, 0.40 and 0.45 V calculated by the Levich equation of the PtAu/C catalyst.

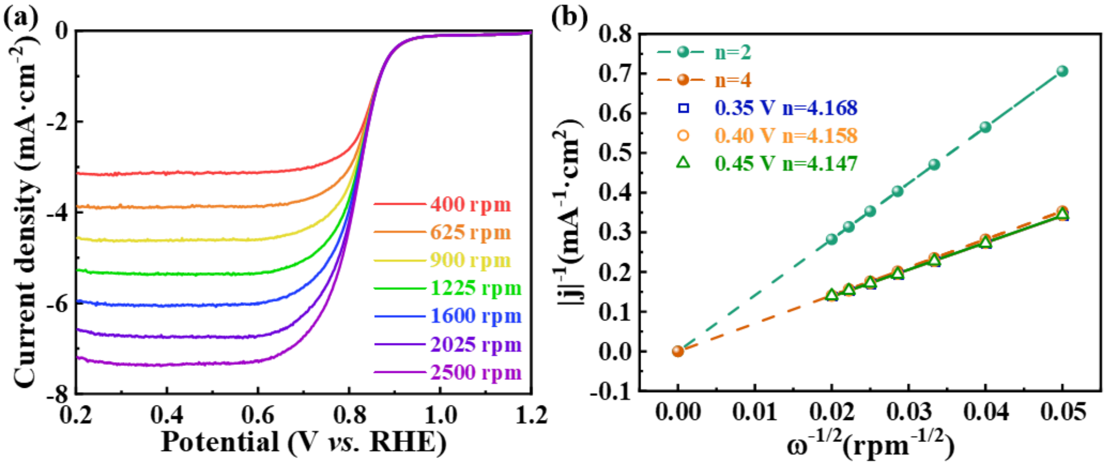

Fig. S6. (a) LSV curves at 400-2500 rpm and (b) transfer electron numbers at 0.35, 0.40 and 0.45 V calculated by the Levich equation of the PtPd/C catalyst.

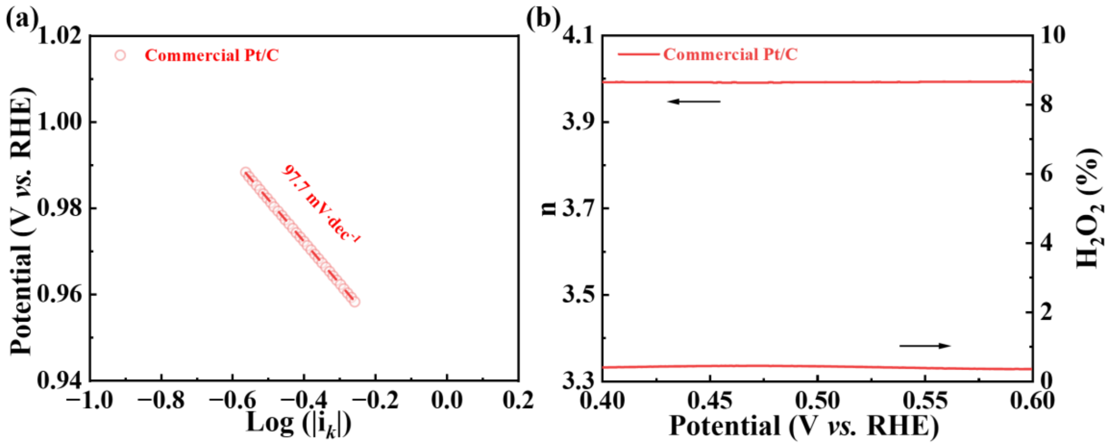

Fig. S7. (a) Initial Tafel slope and (b) transfer electron number n as well as hydrogen peroxide yield of commercial Pt/C catalyst.

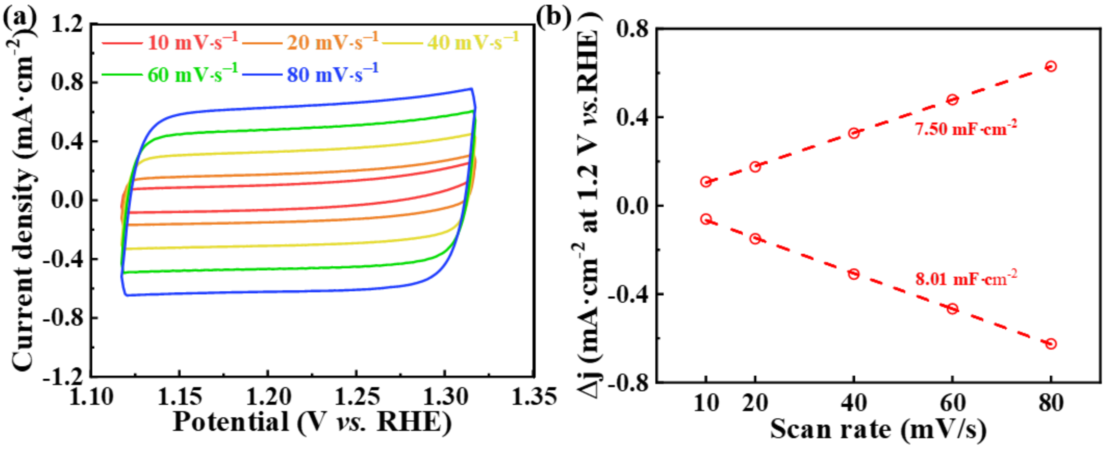

Fig. S8. (a) The CV curves measured in 0.1 M KOH at the scan rates of 10, 20, 40, 60 and 80 mV s^{-1}, and (b) C_{dl} fitting curves of PtAu/C.

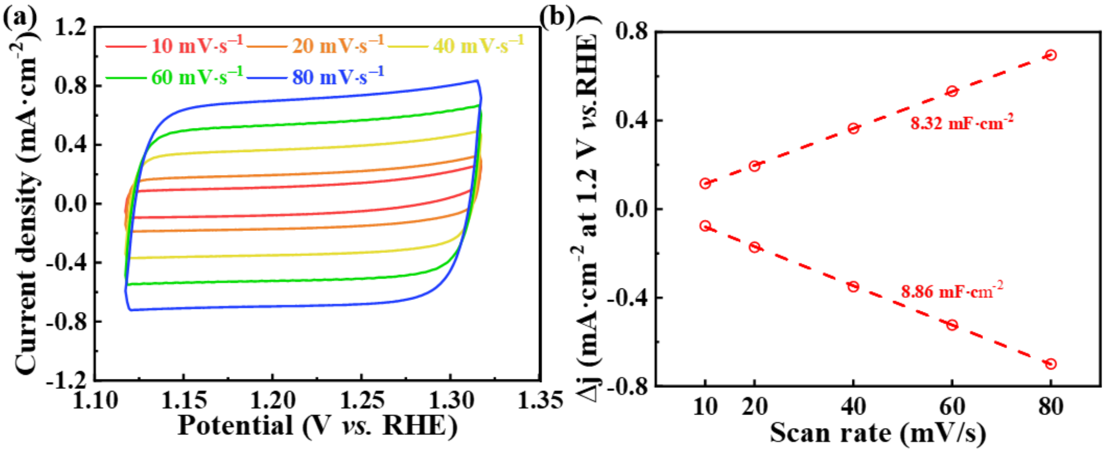

Fig. S9. (a) The CV curves measured in 0.1 M KOH at the scan rates of 10, 20, 40, 60 and 80 mV s^{-1}, and (b) C_{dl} fitting curves of PtPd/C.

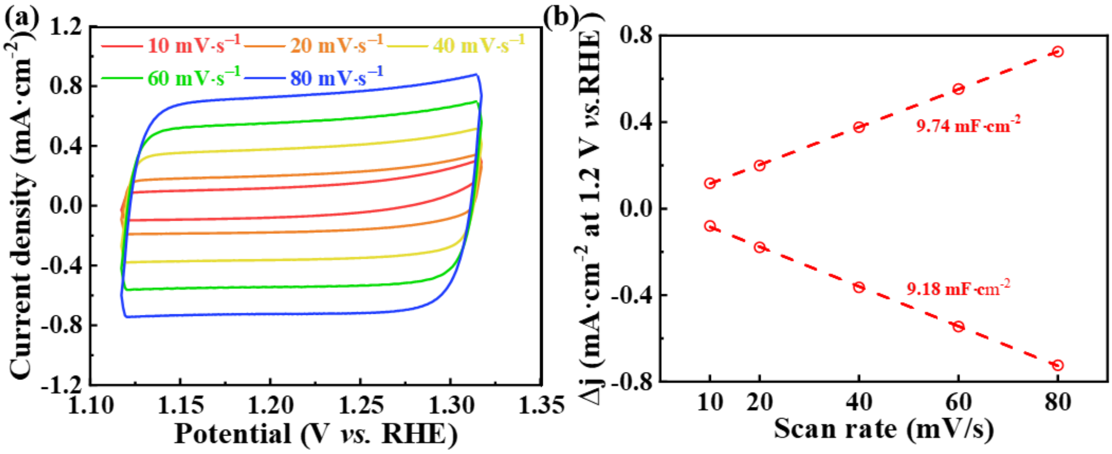

Fig. S10. (a) The CV curves measured in 0.1 M KOH at the scan rates of 10, 20, 40, 60 and 80 mV s^{-1}, and (b) C_{dl} fitting curves of PtAuPd/C.

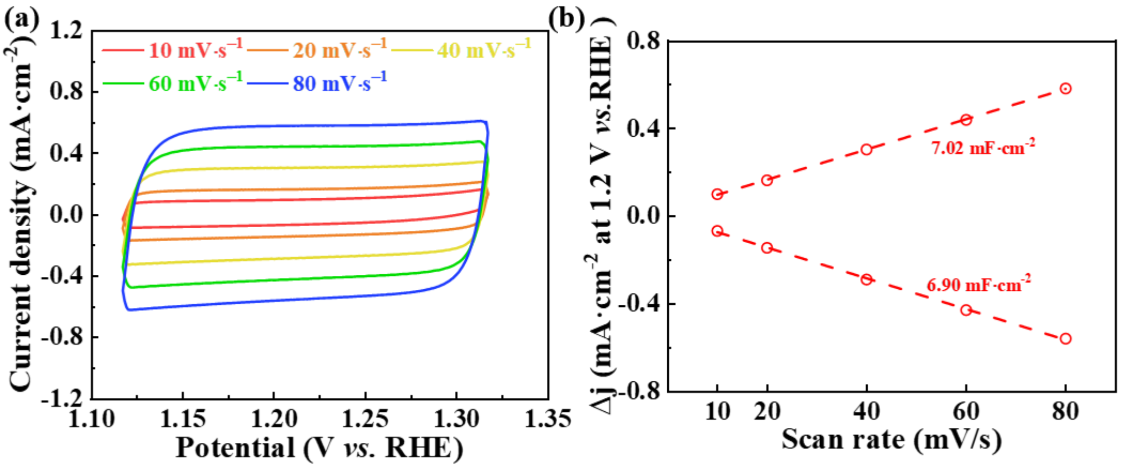

Fig. S11. (a) The CV measured in 0.1 M KOH at the scan rates of 10, 20, 40, 60 and 80 mV s^{-1}, and (b) C_{dl} fitting curves of commercial Pt/C catalyst.

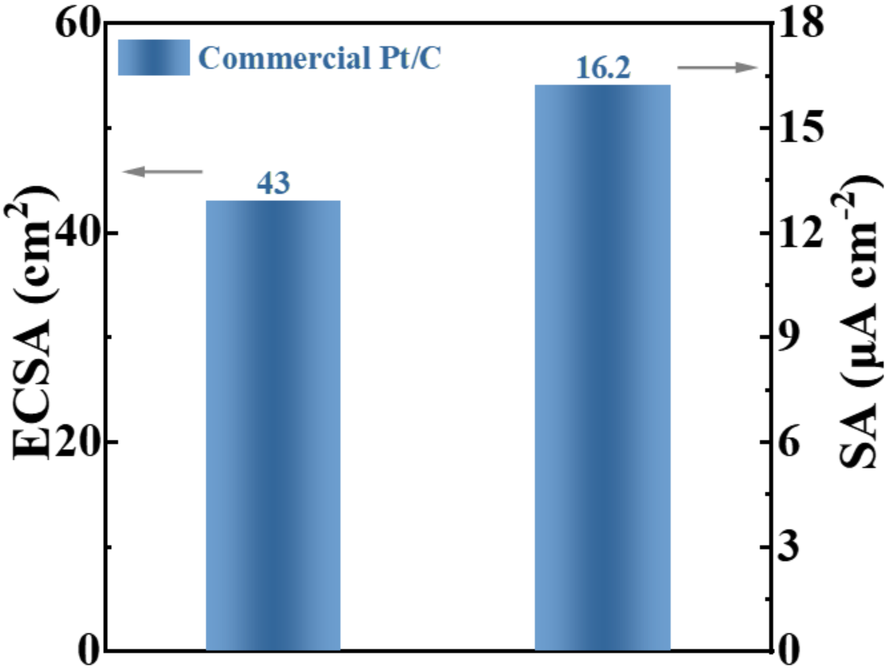

Fig. S12. Electrochemical active area and specific activity of commercial Pt/C catalyst.

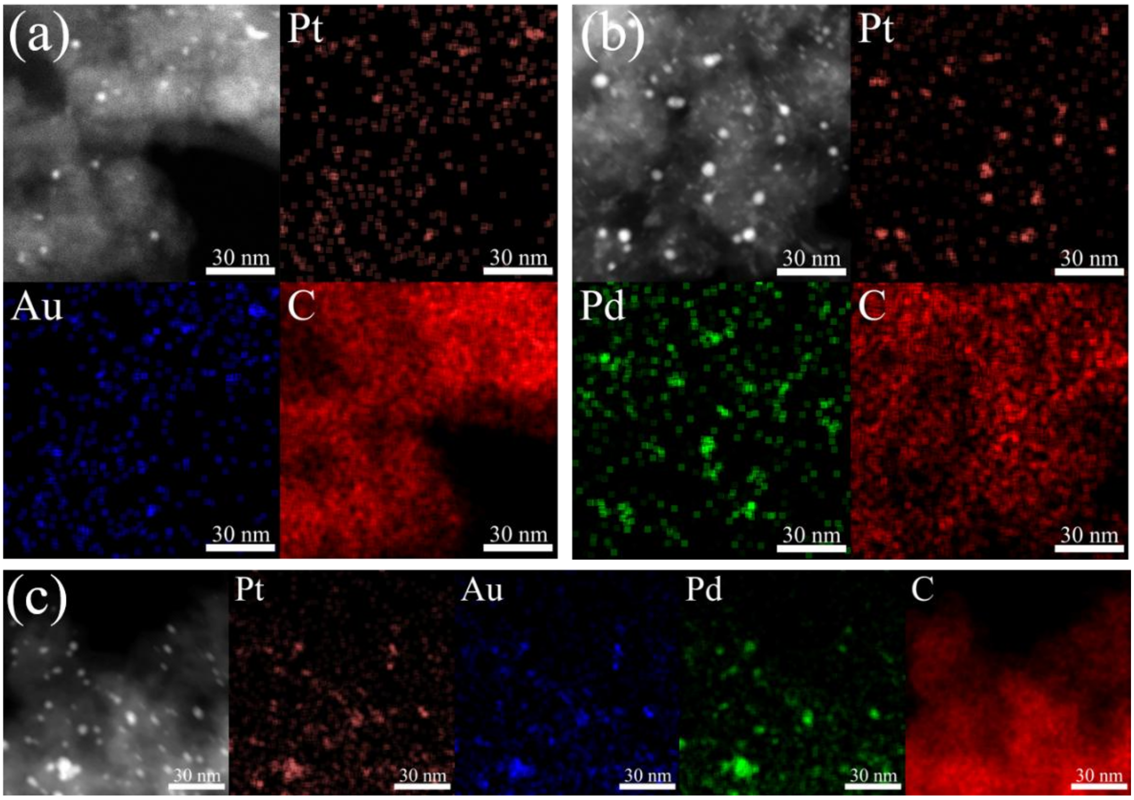

Fig. S13. Mapping element distribution diagrams of (a) PtAu/C, (b) PtPd/C and (c) PtAuPd/C after ADT test.

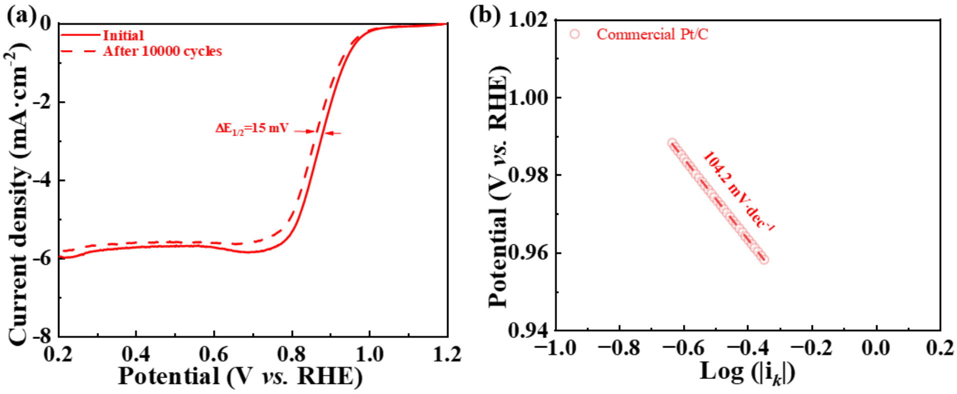

Fig. S14. (a) LSV curves of commercial Pt/C catalyst in the initial state and after accelerated durability testing measured at a scan rate of 10 mV s^{-1} under 1600 rpm, (b) the Tafel slope after ADT test of commercial Pt/C catalyst.

Reference

1. L. Kuang, L. Zhang, S. Lü, J. Wei, Y. Zhou, H. Qin, J. He, Z. Zhang, H. Ni and Y. He, *Atomically dispersed high-loading Pt-Fe/C metal-atom foam catalyst for oxygen reduction in fuel cells*, *J. Alloys Compd.*, 2024, **973**, 172928.
2. Y. Zang, D.-Q. Lu, K. Wang, B. Li, P. Peng, Y.-Q. Lan and S.-Q. Zang, *A pyrolysis-free Ni/Fe bimetallic electrocatalyst for overall water splitting*, *Nat. Commun.*, 2023, **14**(1), 1792.
3. S. Franz, H. Arab, G. L. Chiarello, M. Bestetti and E. Selli, *Single‐Step Preparation of Large Area TiO_2 Photoelectrodes for Water Splitting*, *Adv. Energy Mater.*, 2020, **10**, 2000652.
4. W. Chen and S. Chen, *Oxygen electroreduction catalyzed by gold nanoclusters: strong core size effects*, *Angew. Chem. Int. Ed. Engl.*, 2009, **48**(24), 4386-4389.
5. D. Voiry, M. Chhowalla, Y. Gogotsi, N. A. Kotov, Y. Li, R. M. Penner, R. E. Schaak and P. S. Weiss, *Best Practices for Reporting Electrocatalytic Performance of Nanomaterials*, *ACS Nano*, 2018, **12**(10), 9635-9638.
6. R. Zhou, Y. Zheng, M. Jaroniec and S.-Z. Qiao, *Determination of the Electron Transfer Number for the Oxygen Reduction Reaction: From Theory to Experiment*, *ACS Catal.*, 2016, **6**(7), 4720-4728.